JOC Article

Synthesis and Structural Investigation of New Triptycene-Based Ligands: En Route to Shape-Persistent Dendrimers and Macrocycles with Large Free Volume

Jonathan H. Chong and Mark J. MacLachlan*

Department of Chemistry, University of British Columbia, 2036 Main Mall, Vancouver, BC, V6T 1Z1, Canada

mmaclach@chem.ubc.ca

Received June 18, 2007

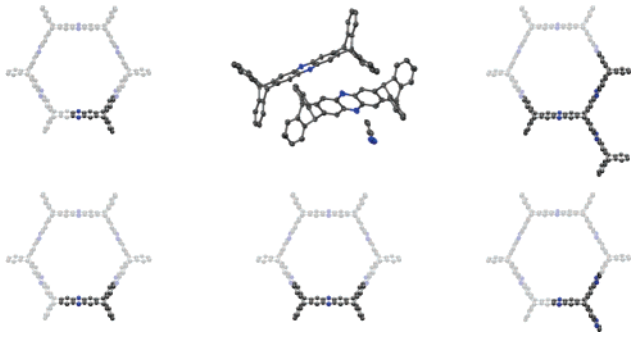

Triptycene was used to build a series of ligands containing pyrazine groups for use in forming coordination frameworks and as model compounds toward target shape-persistent dendrimers and macrocycles. The phenylenediamine precursors are formed by controlled double nitration/reduction of triptycene, followed by condensation with triptycenyl *o*-quinone to form the ligands. Solid-state structures show that the ligands favor packing in layered structures with intermolecular π stacking. Increasing the length of the wings still allows for effective packing, but increasing the number of pyrazine groups or adding more triptycenyl moieties reduces packing efficiency. To demonstrate the potential of these molecules to function as ligands, a coordination complex of **15** with copper(I) iodide was obtained and found to form dimers that pack into a layered arrangement.

Introduction

Rigid shape-persistent macrocycles such as porphyrins, phthalocyanines, and phenyleneethynylenes have emerged as important substances for the study of aggregation and liquid crystallinity.[1] Over the past three decades, many strategies have been developed to synthesize large shape-persistent macrocycles, and most involve the incorporation of conjugated components. This typically results in a planar framework where the orbitals involved in conjugation are directed perpendicularly above and below the plane of the macrocycle. Another approach to shape-persistent macrocycles involves belt-shaped molecules such as cyclodextrins and cucurbiturils.[2] Belt-shaped molecules can also be designed to incorporate extended conjugation, as seen in the proposed [*n*]cyclacene and cyclo[*n*]phenacene classes of molecules; the conjugated orbitals in these molecules are radially directed.[3]

The organization of shape-persistent macrocycles may create molecule-based nanotubes with advantages over other types of

(1) (a) Balaban, T. S. *Acc. Chem. Res.* **2005**, *38*, 612−623. (b) Elemans, J. A. A. W.; van Hameren, R.; Nolte, R. J. M.; Rowan, A. E. *Adv. Mater.* **2006**, *18*, 1251−1266. (c) Eichhorn, H. *J. Porphyrins Phthalocyanines* **2000**, *4*, 88−102. (d) Hu, J.-S.; Guo, Y.-G.; Liang, H.-P.; Wan, L.-J.; Jiang, L. *J. Am. Chem. Soc.* **2005**, *127*, 17090−17095. (e) Castella, M.; Lopez-Calahorra, F.; Velasco, D.; Finkelmann, H. *Chem. Commun.* **2002**, 2348−2349. (f) Jasat, A.; Dolphin, D. *Chem. Rev.* **1997**, *97*, 2267−2340. (g) van Nostrum, C. F. *Adv. Mater.* **1996**, *8*, 1027−1030. (h) Zhang, J.; Moore, J. S. *J. Am. Chem. Soc.* **1992**, *114*, 9701−9702. (i) Inabe, T. *J. Porphyrins Phthalocyanines* **2001**, *5*, 3−12. (j) Lahiri, S.; Thompson, J. L.; Moore, J. S. *J. Am. Chem. Soc.* **2000**, *122*, 11315−11319. (k) Höger, S.; Bonrad, K.; Mourran, A.; Beginn, U.; Möller, M. *J. Am. Chem. Soc.* **2001**, *123*, 5651−5659. (l) Rosselli, S.; Ramminger, A.-D.; Wagner, T.; Lieser, G.; Höger, S. *Chem.−Eur. J.* **2003**, *9*, 3481−3491.

(2) (a) Szejtli, J. *Pure Appl. Chem.* **2004**, *76*, 1825−1845. (b) Harada, A. *J. Polym. Sci., Part A: Polym. Chem.* **2006**, *44*, 5113−5119. (c) Harada, A. *Acc. Chem. Res.* **2001**, *34*, 456−464. (d) Kim, K.; Selvapalam, N.; Ko, Y. H.; Park, K. M.; Kim, D.; Kim, J. *Chem. Soc. Rev.* **2007**, *36*, 267−279. (e) Lee, J. W.; Samal, S.; Selvapalam, N.; Kim, H.-J.; Kim, K. *Acc. Chem. Res.* **2003**, *36*, 621−630.

10.1021/jo701297q CCC: $37.00
Published on Web 10/11/2007

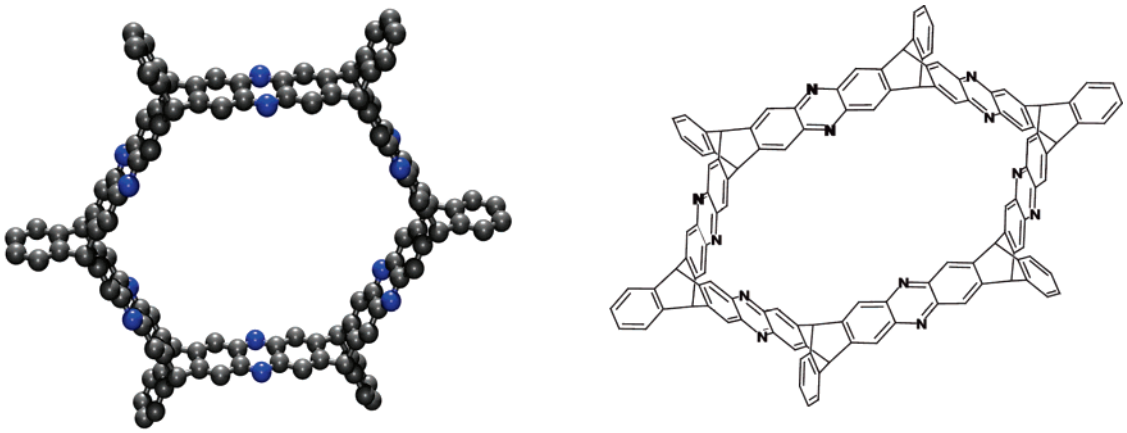

FIGURE 1. Target giant beltlike macrocycle **1**.

SCHEME 1. Synthesis of 2,3-Diaminotriptycene (2)

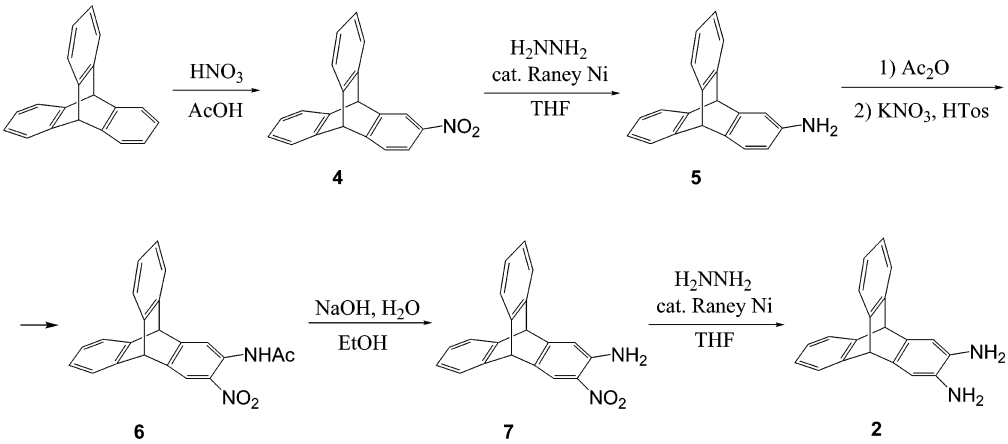

TABLE 1. Product Distributions of Nitrated Triptycenes Formed under Various Reaction Conditions[a]

KNO_3[b]	dinitro[c]	mononitro[c]	triptycene[c]
1	1	7.79	2.09
1.1	1	6.58	1.60
1.2	1	5.12	0.81

[a] All reactions were performed using 0.25 g of triptycene and 1.5 equiv of *p*-toluenesulfonic acid in 10 mL of acetic anhydride, stirring overnight at room temperature. [b] Equivalents of KNO_3 added per equivalent of triptycene used. [c] Ratios of nitrotriptycenes were determined by integration of ^{1}H NMR spectra and are normalized to dinitrotriptycene. Traces of trinitro products evident were not integrated.

nanotubes. For example, although carbon nanotubes possess interesting physical and electronic properties, they are limited by costly and nonintuitive synthetic methods and are difficult to separate.[4] These difficulties have hindered the commercial development of nanotubes for wide-ranging applications. The organization of shape-persistent macrocycles into 1-D tubes offers the possibility of creating uniform, monodisperse nanotubes with homogeneous properties. This approach has been illustrated with the hydrogen-bonded assemblies of cyclic D,L-peptides, which have found use as transmembrane channel mimics.[5] With this molecule-based approach to nanotubes, the size of the tube may be controlled, opening new possibilities for host−guest applications such as selective adsorption, catalysis, and nanowire templation. Furthermore, controlled macrocycle aggregation and de-aggregation would be useful in controlling the adsorption and release of guests and would allow for their eventual removal when used in template-directed synthesis.

We are targeting shape-persistent ligands such as the giant beltlike macrocycle **1** illustrated in Figure 1 for assembly into tubular structures. Phenazine groups on each side of the hexagon could coordinate to metals to link the molecules into a tubular structure or a highly porous 3-D framework.[6] Central to this design of these ligands is the use of triptycene as a thermally robust component. Triptycene is an ideal building block for macrocycle **1** because the constrained 120° angle between the phenyl rings provides the required geometry to form a hexagon.

(3) (a) Tahara, K.; Tobe, Y. *Chem. Rev.* **2006**, *106*, 5274−5290. (b) Ashton, P. R.; Brown, G. R.; Isaacs, N. S.; Giuffrida, D.; Kohnke, F. H.; Mathias, J. P.; Slawin, A. M. Z.; Smith, D. R.; Stoddart, J. F.; Williams, D. J. *J. Am. Chem. Soc.* **1992**, *114*, 6330−6353. (c) Cory, R. M.; McPhail, C. L. *Tetrahedron Lett.* **1996**, *37*, 1987−1990. (d) Neudorff, W. D.; Lentz, D.; Anibarro, M.; Schlüter, A. D. *Chem.−Eur. J.* **2003**, *9*, 2745−2757. (e) Nakamura, E.; Tahara, K.; Matsuo, Y.; Sawamura, M. *J. Am. Chem. Soc.* **2003**, *125*, 2834−2835.

(4) (a) Ajayan, P. M. *Chem. Rev.* **1999**, *99*, 1787−1800. (b) Tasis, D.; Tagmatarchis, N.; Bianco, A.; Prato, M. *Chem. Rev.* **2006**, *106*, 1105−1136.

(5) (a) Ghadiri, M. R.; Granja, J. R.; Milligan, R. A.; McRee, D. E.; Khazanovich, N. *Nature* **1993**, *366*, 324−327. (b) Khazanovich, N.; Granja, J. R.; McRee, D. E.; Milligan, R. A.; Ghadiri, M. R. *J. Am. Chem. Soc.* **1994**, *116*, 6011−6012. (c) Ghadiri, M. R.; Granja, J. R.; Buehler, L. K. *Nature* **1994**, *369*, 301−304. (d) Granja, J. R.; Ghadiri, M. R. *J. Am. Chem. Soc.* **1994**, *116*, 10785−10786. (e) Bong, D. T.; Ghadiri, M. R. *Angew. Chem., Int. Ed.* **2001**, *40*, 2163−2166.

(6) Campbell, K.; Kuehl, C. J.; Ferguson, M. J.; Stang, P. J.; Tykwinski, R. R. *J. Am. Chem. Soc.* **2002**, *124*, 7266−7267.

Extension of triptycene's phenyl rings would then provide an electronic environment where the orbitals involved in conjugation have a similar direction to other conjugated beltlike molecules. The shape of triptycene also hinders packing into dense structures, particularly when appended to larger structures. Along with its derivatives, triptycene has been used to inhibit aggregation in conjugated polymers and to align liquid crystals.[7] Chen has also used triptycene to form crown ether hosts that can complex a variety of ammonium cations.[8]

Munakata has demonstrated that silver(I) can be π-coordinated with triptycene to form extended frameworks.[9] Apart from this, the use of triptycene and its derivatives as ligands for the generation of porous structures is virtually unexplored. We have demonstrated the use of triptycene-based ligands to prepare highly porous 2-D metal−organic frameworks.[10] These structures, formed with CuI, exhibit high chemical and thermal stability and can be used to remove organic impurities from contaminated water. They undergo reversible guest exchange without decomposition of the framework. Coordination of metals to the apical nitrogen atoms of macrocycle **1** could allow for their assembly into stable metal−organic nanotubes with similar properties.

In this paper, we describe the use of triptycenyl *o*-quinone to form a family of shape-persistent ligands. Among the structures prepared, we present a first generation shape-persistent dendrimer and several components of macrocycle **1** that we are targeting. Synthesis, characterization, and structures of the novel phenazine- and quinoxaline-containing compounds are described. These ligands, which incorporate one to four triptycenyl groups, are shape-persistent structures themselves and are promising candidates for the development of robust coordination frameworks with large free volume.

Results and Discussion

Precursors. With the long-term goal of building a shape-persistent macrocycle that could be assembled into a nanotube, we planned to synthesize several quinoxaline- and phenazine-type model compounds that represent portions of the macrocycle. This required us to develop synthetic routes to new triptycenyl precursors such as 2,3-diaminotriptycene (**2**) and 2,3,6,7,14,15-hexaaminotriptycene (**3**).

The best route to compound **2** appeared to be sequential nitration and reduction of one triptycene ring as shown in Scheme 1. Prior kinetic studies of triptycene have shown that the most reactive sites toward electrophilic aromatic substitution are the desired β positions. Nitration on one phenyl ring deactivates it toward further substitution; however, the other two rings are not significantly deactivated, and this leads to a mixture of products. We attempted to optimize the nitration conditions in acetic anhydride to maximize the yield of mononitrotriptycene **4**, with the other byproducts being dinitrotriptycene and unreacted starting material. Table 1 shows the yields of the compounds from several reactions. Adding more KNO_3 reduced the amount of unreacted starting material but led to increased amounts of the undesired dinitrotriptycene; the most desirable method is to use only stoichiometric KNO_3. However, we found that it was faster to use nitric acid in acetic acid combined with heating as this reaction was complete after 6 h.

Compound **4** is difficult to purify by recrystallization, and chromatography is not a suitable technique for scaled-up reactions because the mobility of **4** on silica gel requires dry loading. It is preferable to first reduce the mixture of compounds and then separate **5** from triptycene and diaminotriptycene as all these compounds have significant differences in their mobilities on silica. In situ conversion of the amino group to an acetamide followed by selective nitration at the other β position at low temperature with stoichiometric nitric acid (generated in situ using potassium nitrate and *para*-toluenesulfonic acid) gave compound **6**. Compound **6** was isolated as a yellow solid, and the acetate protecting groups were easily removed by basic hydrolysis to give **7** as an orange-yellow solid. The colors of **6** and **7** arise from the push−pull chromophore between the nitro and amino substituents. Reduction of **7** then afforded air-sensitive **2** as a white crystalline solid in 53% yield.[10]

Hexaaminotriptycene (**3**) has been reported in the literature, prepared by nitration of trinitrotriptycene (45% yield) followed by reduction.[11] The low yield of the nitration is due to the formation of byproducts resulting from reaction at undesired locations under the harsh conditions of the reaction. This is also problematic because the byproducts are similar and are difficult to separate, even by chromatography. To avoid these problems, we synthesized **3** by a sequential double nitration/reduction route analogous to that used to prepare compound **2** (Scheme 2). Triple nitration of triptycene leads primarily to a mixture of two isomers (**8a**,**b**) in an approximate ratio of 3:1 (**8a**:**8b**), which shows that the location of nitration is statistically controlled and not significantly affected by electronic effects. These isomers are difficult to separate by chromatography on a large scale because dry loading is also required and they have similar R_f values. Because both are suitable precursors to **3**, it is possible to carry them through the entire synthetic route without intermediate purification, but this makes purification of the final product more difficult. Therefore, it is preferable to reduce them to the corresponding amines (**9**) and separate the two isomers at this stage by column chromatography. Each amine isomer can then be taken separately through the remainder of the synthetic route to **3**.[10]

Although all of the quinoxaline-type compounds can be synthesized by Schiff base condensation with glyoxal, obtaining the phenazine-type compounds by this synthetic strategy requires *ortho*-quinones. Quinones are typically encountered as the stable *para* species because *o*-quinones are prone to dimerization through a Diels−Alder reaction. *o*-Quinones can be isolated at low temperatures or by incorporating bulky substituents that prevent close approach of two molecules in the orientation required for dimerization to take place.[12] The *o*-quinones we require for our target phenazines must be stable because Schiff base condensations with ketones occur under more forcing conditions with higher temperatures. An *o*-quinone bearing the

(7) (a) Yang, J.-S.; Swager, T. M. *J. Am. Chem. Soc.* **1998**, *120*, 5321−5322. (b) Long, T. M.; Swager, T. M. *Adv. Mater.* **2001**, *13*, 601−604.

(8) (a) Peng, X.-X.; Lu, H.-Y.; Han, T.; Chen, C.-F. *Org. Lett.* **2007**, *9*, 895−898. (b) Zong, Q.-S.; Chen, C.-F. *Org. Lett.* **2006**, *8*, 211−214. (c) Zhu, X.-Z.; Chen, C.-F. *J. Am. Chem. Soc.* **2005**, *127*, 13158−13159.

(9) Munakata, M.; Wu, L. P.; Sugimoto, K.; Kuroda-Sowa, T.; Maekawa, M.; Suenaga, Y.; Maeno, N.; Fujita, M. *Inorg. Chem.* **1999**, *38*, 5674−5680.

(10) Chong, J. H.; MacLachlan, M. J. *Inorg. Chem.* **2006**, *45*, 1442−1444.

(11) (a) Shalaev, V. K.; Skvarchenko, V. R. *Vestn. Mosk. Univ., Ser. 2: Khim.* **1974**, *15*, 726−730. (b) Shalaev, V. K.; Getmanova, E. V.; Skvarchenko, V. R. *Zh. Org. Khim.* **1976**, *12*, 191−197.

(12) Minisci, F.; Citterio, A.; Vismara, E.; Fontana, F.; De Bernardinis, S.; Correale, M. *J. Org. Chem.* **1989**, *54*, 728−731.

SCHEME 2. Synthesis of 2,3,6,7,14,15-Hexaaminotriptycene (3)

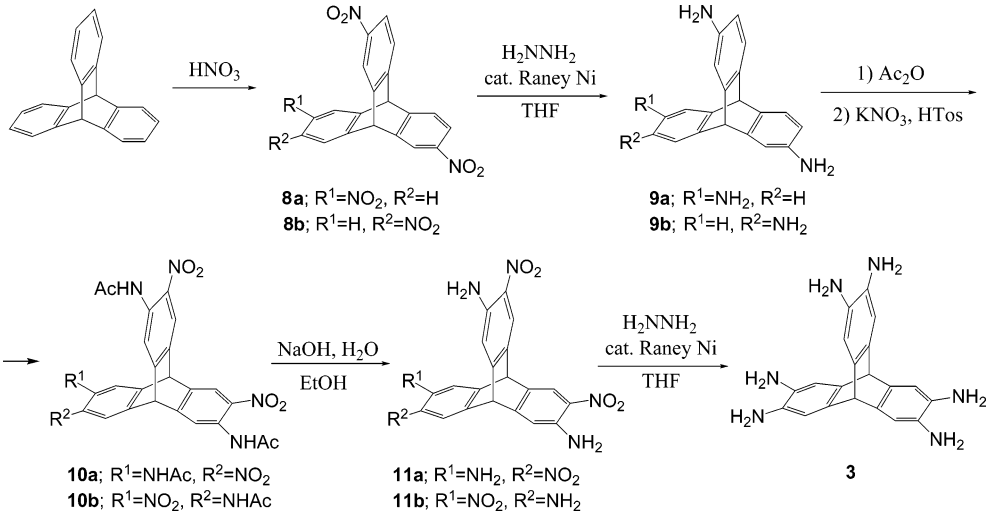

SCHEME 3. Synthesis of Triptycenyl Quinoxaline Ligands 13 and 14

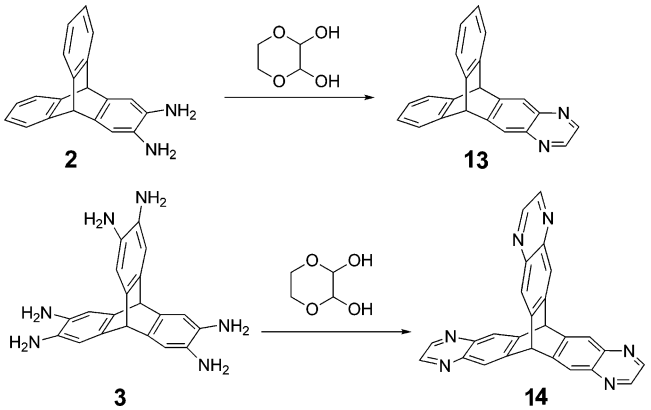

SCHEME 4. Synthesis of Triptycenyl Phenazine Ligands 15−17

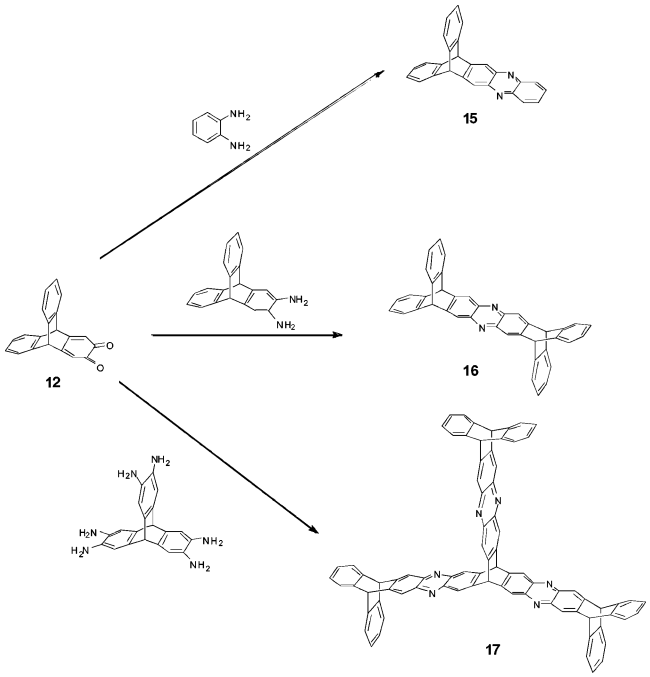

TABLE 2. ^{1}H NMR Resonances of the Bridgehead Protons for Quinoxalines 13 and 14 and Phenazines 15−17

compound	chemical shift (ppm)[a]
13	5.64
14	6.13
15	5.66
16	5.61
17	5.59,[b] 6.05[c]

[a] Calibrated internally to residual $CHCl_3$. [b] Resonance of outer bridgehead protons. [c] Resonance of inner bridgehead protons.

sterically bulky triptycenyl structure (**12**) was recently reported by Chen.[13] Compound **12** is indeed stable at ambient temperatures for months and can be recovered after heating to reflux overnight in ethanol or THF, making it suitable for our use.

Ligands. The quinoxaline-based ligands (**13** and **14**) were synthesized by Schiff base condensation with a glyoxal equivalent that was chosen because of its availability in an anhydrous form (Scheme 3). Ligand **13** is a model compound that represents a vertex and part of a side of the target macrocycle **1**. We expected that these reactions would be essentially quantitative, but the yields were lowered by the formation of unidentified byproducts. In particular, the reaction to form **14** generated a large amount of a poorly soluble oligomeric byproduct. This is surprising because the expected polymer arising from reversible Schiff base condensation should shift toward the thermodynamically stable aromatic quinoxaline. The increased number of amino groups on **3** also increases the possibility for forming a cross-linked polymer that would be difficult to degrade once it precipitates out of solution. Fortunately, it was possible to separate the desired compounds by column chromatography using polar solvent mixtures.

We synthesized the phenazine-type ligands **15** and **16** from quinone **12** (Scheme 4). Ligand **15** is a model compound comprising a vertex and a complete side of macrocycle **1**, and **16** represents a side and two vertices of **1** (Figure 2). THF or THF/ethanol mixtures were initially used as we believed they were necessary for solubility, but this resulted in low product yields. Because ketones react less rapidly than aldehydes, the reaction time was increased but did not produce a corresponding increase in the yield. However, switching to ethanol resulted in

(13) Gong, K.; Zhu, X.; Zhao, R.; Xiong, S.; Mao, L.; Chen, C. *Anal. Chem.* **2005**, *77*, 8158−8165.

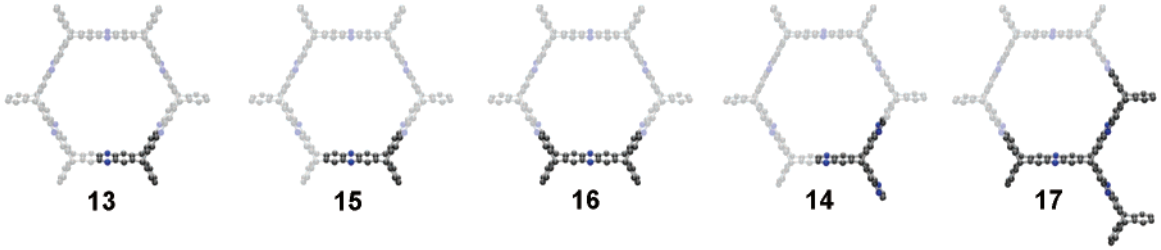

FIGURE 2. Representation of ligands **13**−**17** as model components of macrocycle **1**.

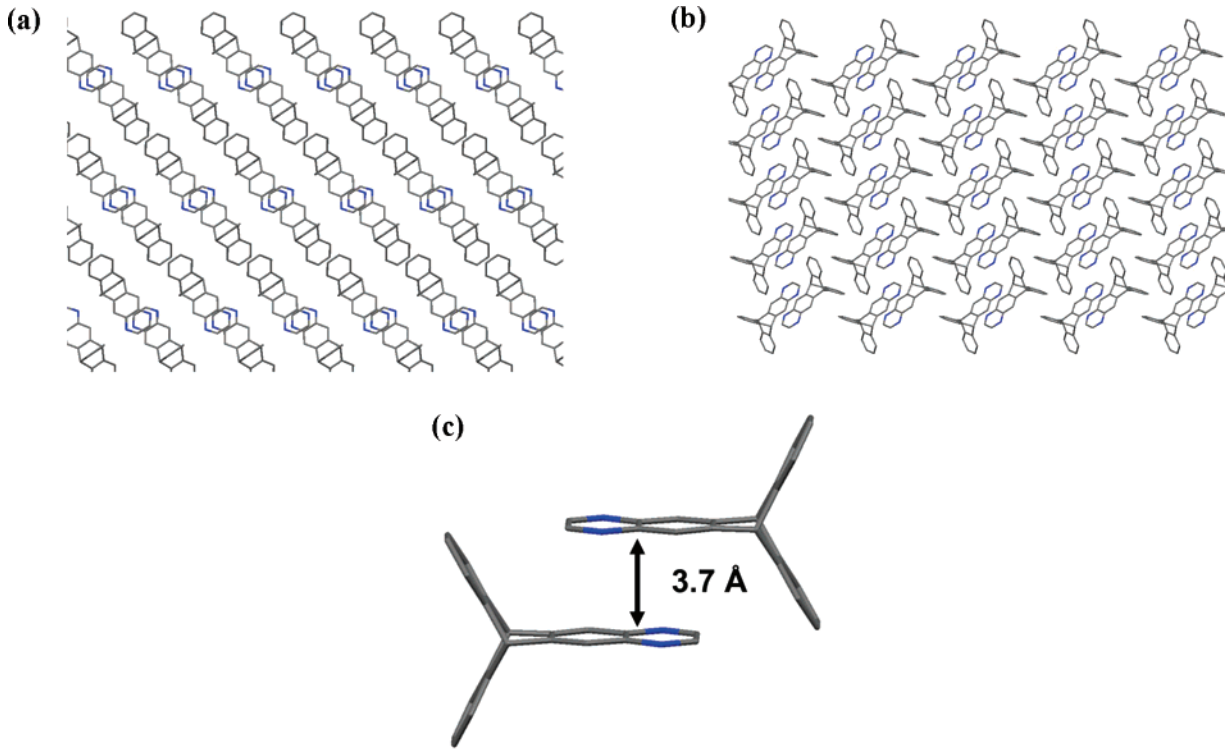

FIGURE 3. Packing arrangement of quinoxaline **13** in the solid state. (a) View along the *a*-axis showing a layered structure. (b) View along the *b*-axis showing interdigitated cofacial assembly. (c) View of π stacked dimers.

reaction mixtures that were easy to purify and gave reasonable yields of 61% and 68% for **15** and **16**, respectively.

Initial attempts to form **17** were particularly problematic as only trace quantities of the desired product were detected. Interestingly, the use of ethanol did not produce a significant improvement as with **15** and **16**. To deal with the possibility of insolubility of the intermediates, we tried THF and THF/ethanol mixtures, but this produced no significant improvement and only resulted in the formation of polymers. Such a polymeric byproduct may be more problematic when a ketone such as **12** is used instead of an aldehyde because the resulting imines would be more stable, making the system less reversible and more difficult to reach the desired thermodynamic product. Fortunately, adding a catalytic amount of piperidine improved the yield of **17** sufficiently to 35%, so that it could be purified and isolated. The base serves as a catalyst for the reaction, making it easier to reverse the formation of unwanted kinetic byproducts. Purification of **17** was facilitated by chromatography with an alumina stationary phase. NMR spectroscopy shows the expected signals and also confirms that there are no impurities present. Notably, the ^{1}H NMR spectrum shows two signals for the bridgehead, at 6.05 and 5.59 ppm for the inner and outer bridgeheads, respectively (Table 2). MALDI-TOF mass spectrometry for **17** shows the expected $[M + H]^+$ ion, without any observable oligomeric or polymeric impurities (see Supporting Information).

The chemical shift of the triptycenyl bridgehead protons is a useful diagnostic feature for all triptycene compounds as it is sensitive to changes on the phenyl rings. For the ligands in this study, the chemical shifts are dependent on the number of substituted phenyl rings adjacent to the bridgehead. Bridgeheads with three adjacent quinoxalines or phenazines have protons that resonate downfield by ca. 0.4 ppm compared to those that only have a single adjacent quinoxaline or phenazine. This can be seen in the chemical shifts for **17**; the protons on its inner bridgehead resonate 0.46 ppm downfield of those on its outer bridgeheads. Although sensitive to the number of substitutions, the chemical shift is not significantly affected by the presence of a quinoxaline versus a phenazine moiety.

Structures. To study how changes in the structure of the ligands affected their packing in the solid state, we undertook single-crystal X-ray diffraction experiments of **13**−**16**. In the solid state, quinoxaline **13** packs into a layered structure, and within each layer the molecules show interdigitated cofacial assembly (Figure 3). The pyrazine ring lies over top of the phenyl ring on the other molecule with a separation of 3.7 Å;

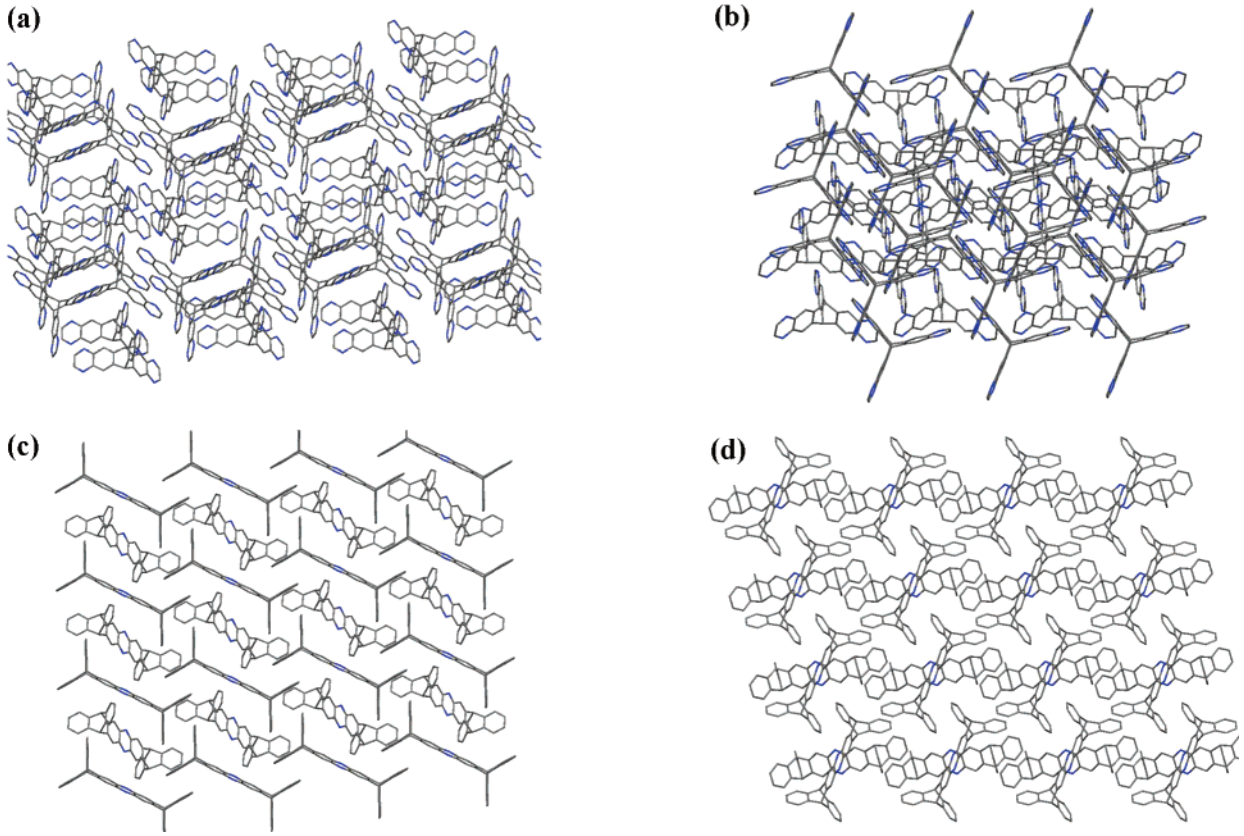

FIGURE 4. Packing arrangements of trisquinoxaline **14** and phenazine **16** in the solid state. Guest solvent molecules have been omitted for clarity. (a) View of **14** crystallized from MeCN showing orthogonal layers and π stacking. (b) View of **14** crystallized from THF showing the presence of layers with two different orientations. (c) View of **16** along the *a*-axis. (d) View of **16** along the *b*-axis.

this allows for weak π stacking between pairs of molecules within each layer. This appears to be a relatively efficient packing arrangement, as there are no guest solvent molecules in the lattice, and the structure has a calculated density of 1.35 g/cm^3.

Crystals of trisquinoxaline **14** were obtained from two different solvents, MeCN and THF. The structure of **14** crystallized from MeCN contains 12 guest acetonitrile molecules per unit cell (1.5 molecules of MeCN per molecule of **14** as one MeCN lies on a mirror plane) (Figure 4a). This structure contains two layers orientated orthogonally to each other. A similar π stacking arrangement, with the phenyl ring being over top of the pyrazine ring separated by 3.6 Å, can be seen between pairs of adjacent molecules within the same layer. This packing arrangement of the quinoxaline is sufficiently poor that there is space to accommodate MeCN in the lattice. Interestingly, the solid-state structure of **14** crystallized from THF is completely different (Figure 4b). In this structure, there is no guest solvent in the lattice. This solvent-free structure has two layers that are twisted with respect to each other by roughly 30°, allowing for a more efficient filling of space. However, this geometry does not allow for the π stacking interactions that may have been required to stabilize the more loosely packed form obtained from MeCN. The structure of **14** crystallized from MeCN has a calculated density of 1.20 g/cm^3 (1.38 g/cm^3 with the presence of solvent guests), whereas crystallizing from THF gives a higher density of 1.42 g/cm^3.

The smallest triptycenyl phenazine (**15**) packs into a layered structure with interdigitated cofacial assembly within each layer, which is similar to the structure for **13** (see Supporting Information). Again, there is weak π stacking between pairs of molecules in the same layer with a separation of 3.8 Å. Ligand **15** differs from **13** as the pyrazine rings in **15** stack directly on top of each other and not over top of the adjacent phenyl rings. This form of packing leads to minimal free space in the lattice (calculated density of 1.34 g/cm^3), with no guest solvent, demonstrating that lengthening one of the wings has little effect on solid-state packing efficiency.

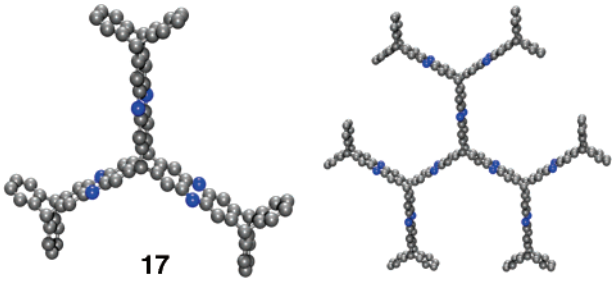

FIGURE 5. First (**17**) and second generations of the proposed triptycenyl dendrimer.

However, adding another triptycenyl moiety resulting in a molecule with two sets of triptycenyl wings, as in **16**, produces a significant decrease in the solid-state packing efficiency. It is clear that the structure of this compound would restrict close packing. The molecules are arranged into two layers that are twisted with respect to each other, presumably to fill space more efficiently (Figures 4c and 4d). However, the presence of guest solvent molecules shows that this arrangement is not as efficient, with a calculated density of 1.26 g/cm^3 (1.31 g/cm^3 with the

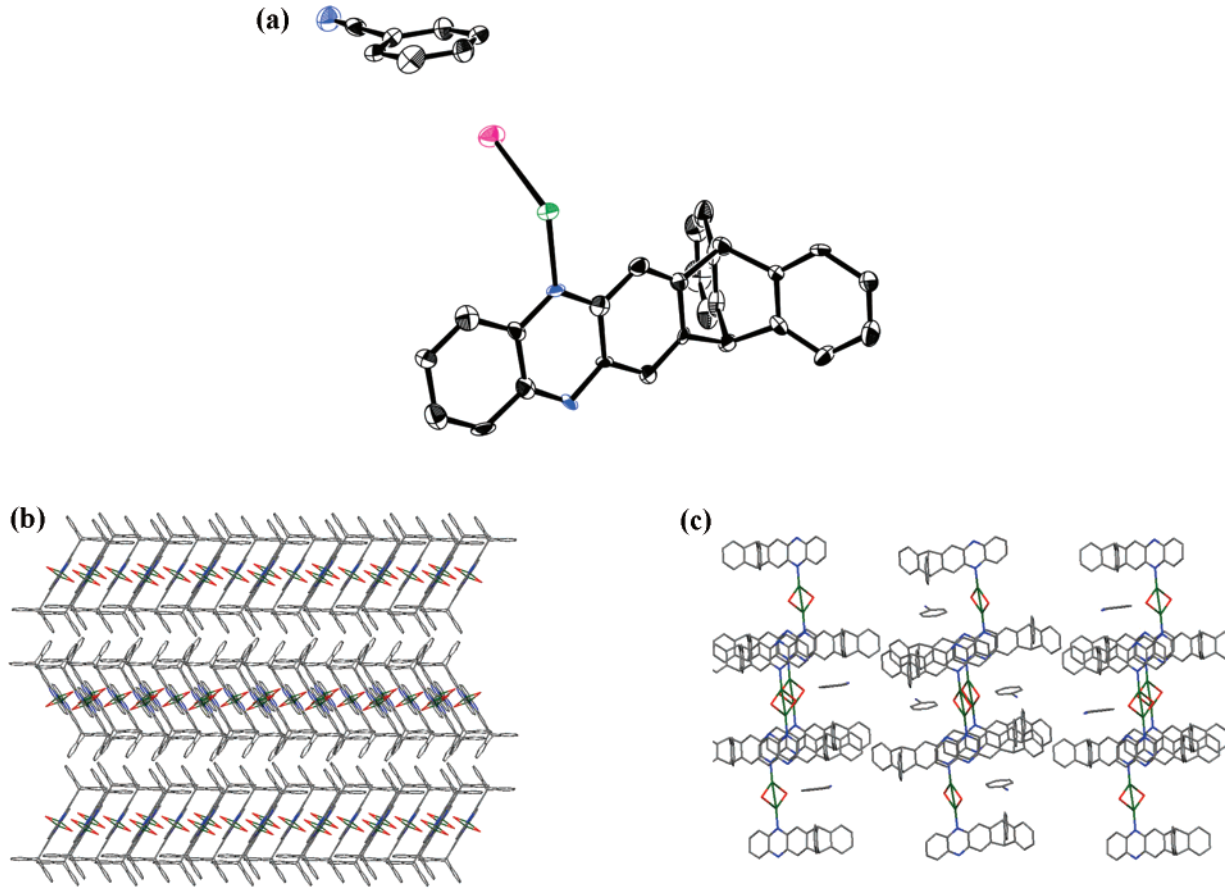

FIGURE 6. Solid-state structure of the **Cu-15** coordination dimer. (a) Asymmetric unit. Ellipsoids are shown at the 50% probability level. Carbon, black; nitrogen, blue; copper, green; iodine, red. (b) View along the *a*-axis showing a herringbone layered structure. Guest solvent molecules have been omitted for clarity. (c) View along the *b*-axis showing solvent-filled voids.

presence of solvent guests). There is also no observed π stacking, as the extra triptycenyl moiety prevents the molecules from approaching each other closely enough with the correct orientation.

Unfortunately, attempts to crystallize **17** have so far been unsuccessful. Compound **17** can also be considered as the first generation of a triptycenyl-based dendrimer (Figure 5); subsequent generations could be synthesized divergently by alternating condensations of aminotriptycenes with triptycenyl quinones. Such dendrimers would also be expected to exhibit poor packing in the solid state, and if the expected void spaces are guest-free, these dendrimers may be useful as low-κ dielectric materials for electronic applications. With a high accessible surface area that is constructed with aromatic rings, the dendrimers may also be promising hydrogen storage materials.

Ligands **13**−**15** were stable to high temperatures of 341, 442, and 378 °C, respectively, while **16** and **17** showed mass losses beginning at 169 and 163 °C, respectively. It appears that thermal stability of these compounds decreases as the number of triptycenyl wings increases. Interestingly, compounds **13** and **15**, with only a single set of wings, essentially have a single decomposition where the entire mass is lost in one step. As the number of triptycenyl wings increases, so does the number of decomposition steps, with **17** appearing to have three stages of mass loss.

The new triptycenyl quinoxaline and phenazine ligands here are potential precursors for forming highly porous, rigid frameworks. We previously found that coordination frameworks from quinoxaline **13** formed with copper(I) iodide.[10] To demonstrate the potential of the new molecules to coordinate to metals, we investigated the reaction of **15** with copper salts. Reaction of **15** with CuI in benzonitrile gave dark red crystals of **Cu-15**. Surprisingly, the structure in this case is not an extended framework but instead is a dimer with two molecules of **15** bridged by Cu_2I_2 (Figure 6). The solid-state packing of **Cu-15** shares some characteristics with its ligand, as it forms a herringbone layered structure with π stacking. The stacked phenazines are separated by 3.6 Å, and they also have the pyrazine rings over top of each other and the phenyl rings on top of each other. Despite the π stacking, the dimers do not pack together very well, with large solvent-filled voids, similar to what is observed for **Cu-13**. The similarity suggests that if the coordination can be extended the expected framework should have a structure similar to **Cu-13**.

AM1 calculations of the target macrocycle **1** show that it should have an inner diameter of 17 Å. While this is likely too large for use in rotaxane chemistry, its size makes it ideal for forming large shape-persistent nanotubes when stacked on top of each other. These nanotubes would possess hydrophobic interiors that should selectively adsorb nonpolar guests. Furthermore, the π stacking interactions from the numerous aromatic rings in **1** would be useful for selectively binding a large number of aromatic guests within the pores. Calculations suggest the interior of macrocycle **1** may be able to bind a single molecule of C_{60} as the intermolecular distances are around 3.7 Å, allowing for $\pi-\pi$ interactions; this behavior has been seen

for similar geometrical motifs.[14] Their assembly into nanotubes could be facilitated by coordination of CuI to the apical nitrogen atoms on the top and bottom edges of the macrocycle, similar to what has been observed for **Cu-13**, **Cu-14**, and **Cu-15**.[10] Incorporation of CuI is expected to maintain the hydrophobicity of the macrocycle, ideal for nonpolar guests. Moreover, metal coordination is expected to assist in holding the nanotubes together and should increase their rigidity and make them more robust.

Conclusions

We have successfully synthesized a series of triptycene-based ligands containing pyrazine groups for use in forming coordination frameworks and as model compounds toward target shape-persistent dendrimers and macrocycles. Their packing arrangement in the solid state has been studied by X-ray crystallography, and it was found that an increase in the number of triptycene groups disrupted intermolecular interactions that lead to efficient packing. We have also synthesized a rigid, shape-persistent first generation dendrimer based on this chemistry. We will continue to expand our library of triptycenyl ligands and further investigate their use in forming coordination frameworks.

Experimental Section

Synthesis of Triptycene Quinoxaline 13. To a solution of compound **2** (0.814 g, 2.86 mmol) in THF (150 mL) was added 2,3-dihydroxy-1,4-dioxane (0.391 g, 3.26 mmol). The solution was stirred under N_2 overnight to give a yellow solution. The solvent was removed by rotary evaporation, and the red-orange residue was chromatographed on silica gel with 1:9 ethyl acetate:dichloromethane to give the product as an off-white solid (0.587 g, 67% yield). ^{1}H NMR (300 MHz, $CDCl_3$) δ 8.70 (s, 2H), 7.99 (s, 2H), 7.47−7.44 (m, 4H), 7.07−7.04 (m, 4H), 5.64 (s, 2H) ppm; ^{13}C NMR (75.4 MHz, $CDCl_3$) δ 146.7, 144.2, 143.7, 142.0, 126.0, 124.1, 122.9, 53.6 ppm; MS (EI, 70 eV) *m*/*z* 305 (M^+); IR ν (KBr) = 3423, 3056, 2959, 1470, 1459, 1433, 1364, 1174, 1157, 1069, 1029, 940, 899, 769, 742, 629, 577, 496 cm^{-1}; mp > 300 °C. Anal. Calcd for $C_{22}H_{14}N_2$: C, 86.25; H, 4.61; N, 9.14. Found: C, 85.90; H, 4.78; N, 9.41.

Synthesis of Triptycene Quinoxaline 14. To a solution of compound **3** (0.319 g, 0.93 mmol) in THF (120 mL) was added 2,3-dihydroxy-1,4-dioxane (0.334 g, 2.78 mmol). The solution was stirred under N_2 overnight to give an orange solution. The solvent was removed by rotary evaporation, and the brown residue was chromatographed on silica gel with 1:9 methanol:dichloromethane to give the product as an off-white solid (0.112 g, 29% yield). ^{1}H NMR (300 MHz, $CDCl_3$) δ 8.76 (s, 6H), 8.21 (s, 6H), 6.13 (s, 2H); ^{13}C NMR (75.4 MHz, $CDCl_3$) δ 144.9, 143.7, 142.2, 124.4, 52.8 ppm; MS (EI, 70 eV) *m*/*z* 410 (M^+); IR ν (KBr) = 3433, 3047, 1474, 1430, 1366, 1176, 1078, 1025, 934, 901, 747, 577 cm^{-1}; mp > 300 °C. Anal. Calcd for $C_{26}H_{14}N_6$: C, 76.09; H, 3.44; N, 20.48. Found: C, 75.87; H, 3.57; N, 20.36.

(14) (a) Kawase, T.; Kurata, H. *Chem. Rev.* **2006**, *106*, 5250−5273. (b) Veen, E. M.; Feringa, B. L.; Postma, P. M.; Jonkman, H. T.; Spek, A. L. *Chem. Commun.* **1999**, 1709−1710.

Synthesis of Triptycene Phenazine 15. To a flask containing *o*-phenylenediamine (0.050 g, 0.46 mmol) and **12** (0.150 g, 0.53 mmol) was added degassed ethanol (30 mL). The solution was refluxed under N_2 for 1.5 h, and the solvent was removed by rotary evaporation. Column chromatography of the residue on silica gel with CH_2Cl_2 yielded the desired product as a pale yellow solid (0.101 g, 61% yield). ^{1}H NMR (300 MHz, $CDCl_3$) δ 8.17−8.14 (m, 2H), 8.07 (s, 2H), 7.75−7.72 (m, 2H), 7.50−7.48 (m, 4H), 7.10−7.08 (m, 4H), 5.66 (s, 2H) ppm; ^{13}C NMR (75.4 MHz, $CDCl_3$) δ 146.6, 143.2, 143.0, 142.9, 129.8, 129.4, 126.2, 124.1, 122.4, 53.5 ppm; MS (EI, 70 eV) *m*/*z* 356 (M^+); IR ν (KBr) = 3430, 3072, 3039, 2954, 1526, 1461, 1429, 1357, 1319, 1203, 1180, 1159, 1130, 1025, 1002, 886, 859, 801 cm^{-1}; mp > 300 °C. Anal. Calcd for $C_{26}H_{16}N_2$: C, 87.62; N, 7.86; H, 4.52. Found: C, 87.44; N, 7.81; H, 4.61.

Synthesis of Triptycene Phenazine 16. To a flask containing **2** (0.100 g, 0.35 mmol) and **12** (0.110 g, 0.39 mmol) was added degassed ethanol (50 mL). The solution was refluxed under N_2 for 1.5 h, and the solvent was removed by rotary evaporation. Column chromatography of the residue on silica gel with CH_2Cl_2 yielded the desired product as a pale yellow solid (0.128 g, 68% yield). ^{1}H NMR (300 MHz, $CDCl_3$) δ 8.00 (s, 4H), 7.47−7.44 (m, 8H), 7.07−7.05 (m, 8H), 5.61 (s, 4H) ppm; ^{13}C NMR (75.4 MHz, $CDCl_3$) δ 145.8, 143.4, 142.3, 126.1, 124.1, 122.4, 53.5 ppm; MS (EI, 70 eV) *m*/*z* 532 (M^+); IR ν (KBr) = 3071, 3037, 2955, 1530, 1461, 1425, 1347, 1315, 1245, 1210, 1201, 1166, 1157, 1071, 1026, 878, 799, 763, 754, 739, 724 cm^{-1}; mp > 300 °C. Anal. Calcd for $C_{40}H_{24}N_2$: C, 90.20; N, 5.26; H, 4.54. Found: C, 89.87; N, 5.66; H, 4.73.

Synthesis of Triptycene Phenazine 17. To a flask containing **3** (0.025 g, 0.07 mmol) and **12** (0.100 g, 0.35 mmol) was added a degassed mixture of ethanol (40 mL) and 6 drops of piperidine. The solution was refluxed overnight under N_2, and the solvent was removed by rotary evaporation. Chromatography of the residue on an alumina column with 1:9 EtOAc:CH_2Cl_2 gave the desired product as a pale yellow solid (0.028 g, 35% yield). ^{1}H NMR (300 MHz, $CDCl_3$) δ 8.23 (s, 6H), 7.99 (s, 6H), 7.45−7.41 (m, 12H), 7.06−7.03 (m, 12H), 6.05 (s, 2H), 5.59 (s, 6H) ppm; ^{13}C NMR (75.4 MHz, $CDCl_3$) δ 146.4, 143.2, 142.75, 142.69, 142.4, 126.2, 124.1, 124.0, 122.4, 53.5, 52.9 ppm; MS (MALDI, dithranol) *m*/*z* 1089.7 ($[M + H]^+$); IR ν (KBr) = 3438, 3072, 3043, 3024, 2961, 1526, 1492, 1459, 1422, 1348, 1271, 1223, 1160, 883, 733 cm^{-1}; mp > 300 °C. Anal. Calcd for $C_{80}H_{44}N_6 \cdot 2H_2O$: C, 85.39; N, 7.47; H, 4.30. Found: C, 85.59; N, 7.52; H, 4.48.

Synthesis of Coordination Dimer Cu-15. A mixture of **15** and copper(I) iodide in benzonitrile was refluxed for 2 h. Slow cooling to room temperature afforded dark red crystals of suitable quality for X-ray diffraction. Anal. Calcd for $C_{73}H_{47}N_2Cu_2I_2$ (**Cu-15**·3PhCN [composition confirmed by TGA]): C, 62.49; N, 6.99; H, 3.38. Found: C, 62.48; N, 6.92; H, 3.48.

Acknowledgment. We thank NSERC of Canada for funding. J.H.C. thanks NSERC for a PGSD graduate fellowship. We also thank Brian Patrick for assistance with XRD.

Supporting Information Available: General experimental details, NMR spectra, TGA curves, and X-ray diffraction data (CIF). This material is available free of charge via the Internet at http://pubs.acs.org.

JO701297Q